Available online at www.sciencedirect.com

SciVerse ScienceDirect

Ceramics International 38 (2012) 5513–5519

CERAMICS INTERNATIONAL

www.elsevier.com/locate/ceramint

Effect of the spark plasma sintering (SPS) parameters and LiF doping on the mechanical properties and the transparency of polycrystalline Nd-YAG

N. Frage, S. Kalabukhov, N. Sverdlov, V. Kasiyan, A. Rothman *, M.P. Dariel

Department of Materials Engineering, Ben-Gurion University of the Negev, Beer-Sheva, Israel

Received 2 February 2012; received in revised form 11 March 2012; accepted 27 March 2012
Available online 6 April 2012

Abstract

Transparent 1 at.% Nd:YAG ceramics were fabricated by spark plasma sintering (SPS) from nanometric Nd:YAG powders, both undoped and pre-mixed with 0.25 wt.% LiF additive. The mechanical and optical properties of the consolidated samples were determined as a function of the processing parameters, namely holding time, peak sintering temperature and heating rate. The presence of LiF accelerates densification and grain growth. Hardness and bending strength are decreased in the presence of the LiF additive, in consistence with the increase of the grain size. The optical transmittance in the doped samples sintered at 1400 °C, reaches 97% of the theoretical transmission and is significantly higher than that of the undoped samples. The increased optical transmittance of the doped samples is attributed to pore elimination by enhanced mass transport and cleansing of the carbon contamination by the fluorine component of the LiF additive. The presence of the latter has no effect on the absorption spectrum of the Nd:YAG ceramic.

Keywords: B. Grain size; C. Mechanical properties; Nd:YAG; Spark plasma sintering; Optical transmittance

1. Introduction

Transparent ceramics are finding an ever-increasing role as advanced structural and functional materials. The multi-faceted applications of transparent ceramics have given rise to a wide spectrum of investigations, aimed at optimizing manufacturing procedures. Among the latter, electric field driven sintering, often denoted spark plasma sintering (SPS), has gained great popularity over the past decade. Spark plasma sintering has now been reviewed [1] and is used in many laboratories over the world. One of its advantages lies in the high turnover of results providing convenient rapid feed-back in the R&D stage of new processes.

Among the various transparent ceramics, subject to increasing demand, yttrium aluminum garnet (YAG) is conspicuously present. YAG and its numerous doped derivatives find a multitude of civilian and military applications [2–4]. Initially utilized in single crystal mode, associated with an expensive manufacturing procedure, YAG is currently processed using powder technological techniques, yielding a polycrystalline material with properties on par with those of single crystals. The commonly used procedure for the fabrication of polycrystalline YAG consists of sintering, with or without external pressure, followed by hot isostatic pressing (HIP) [5]. This procedure allows obtaining high optical quality transparent YAG with a 1–2 μm grain size.

The use of SPS for the fabrication of transparent YAG has also been examined over the past years [6,7]. In most reported SPS-based processing studies of YAG ceramics, the efforts were directed towards achieving full density and determining the effect of the SPS process parameters on the final grain size. Nearly theoretical density was achieved in most cases, but the optical transparence results were mostly disappointing, in particular in the UV and visible wave-length region of the spectrum. For instance, Chaim et al. [7,8] reported on the high density level that was achieved, while optical transparency of the specimens was rather poor and far from the theoretical value. This effect was attributed to the presence of residual pores [7,9].

Frage et al. [6] starting from nano-sized powder and in the presence of 0.25 wt.% LiF additive succeeded in obtaining SPS processed YAG samples with transparency close to the

* Corresponding author. Tel.: +972 52 3644267.
E-mail address: rothmana@bgu.ac.il (A. Rothman).

0272-8842/$36.00
http://dx.doi.org/10.1016/j.ceramint.2012.03.066

theoretical limit. The effect of LiF additive on the densification rate and grain growth in the course of sintering magnesium aluminate spinel and YAG nano-powders was discussed in our previous communications [10,11]. Its presence has also a far reaching effect on the transparency by eliminating the unavoidable carbon contamination in the SPS environment. Recently, the effect of the LiF additive on the quality of SPS processed yttrium oxide (Y_2O_3) has been examined by Marder et al. [12]. The authors confirmed the accelerated sintering effect of the LiF additive, but their results revealed a rather non-homogeneous microstructure of Y_2O_3, SPS-treated samples over a wide temperature range (from 1000 to 1500 °C). They also reported the presence of residual LiF segregated at grain boundaries.

Neodymium YAG (Nd:YAG) based lasers are wide-spread having found applications in medicine, dentistry, metal manufacture and military hardware [13]. The method of preparation and the optical properties of transparent ceramics, manufactured by sintering Nd:YAG nano-powders as starting material, have been reported by several authors [2,3,14]. These ceramics were characterized by micro-sized grains and their optical properties were almost identical to those reported for single crystal Nd:YAG. Fully dense Nd:YAG ceramics have been obtained by conventional sintering at elevated temperature above 1700 °C in the presence of a silica additive [15,16]. The effect of pressure application on the grain size of Nd:YAG following SPS treatment was reported in [17]. The relationship between the microstructural characteristics and the performance of Nd:YAG lasers has been discussed elsewhere [18].

Whereas quasi unanimity prevails regarding the beneficial effect of nano-crystalline starting powder, much uncertainty surrounds various SPS parameters. In particular, no agreement exists regarding the heating rate, the presence, nature and effect of the additives, the optimal grain size which provides sufficient transparency and adequate mechanical properties. The issue of the heating rate, in particular, has not been yet fully resolved on account of the conflicting effect its exerts on the grain growth and densification. Morita et al. [19,20] stressed the importance of a low heating rate of the spinel nano-powder for obtaining nano-sized fully dense specimens with improved transparency. In contrast, Rachman [8] pointed out that a low heating rate favors undesirable grain growth at low temperatures and thereby, promotes the formation of large pores that are difficult to eliminate.

The successful use of the SPS technique for the fabrication of transparent ceramics entails optimization of the SPS processing parameters, namely temperature, heating rate, holding time and applied pressure profile. The resulting products have to be characterized with regard to their microstructure, essentially, the grain size and its distribution, the presence of pores or second any phases. In Nd:YAG optical parameters are of paramount importance, for other transparent ceramics, e.g. spinel, structural properties, mainly mechanical properties are also of great relevance. It is also important to point out that the SPS processing parameters may affect in different ways different properties. A certain set of parameters provides desired mechanical properties, whereas a different set allows achieving best transparency. As a consequence, the ultimate choice of the processing parameters depends on the functionality required from the product material.

Considering the successful manufacture by the SPS treatment of YAG with a high level of optical transparence in the presence of the LiF additive, it was of obvious interest to examine this approach for the fabrication of Nd:YAG. The present communication aims to correlate the functional characteristics of SPS-processed specimens with the SPS processing parameters and to determine whether the presence of LiF additive affects their functional properties.

2. Experimental procedure

Neodymium (1 at.%)-doped yttrium aluminum garnet powder with 50 nm particle size (Nanocerox, Inc.) was used in this study. The Nd:YAG powder was immersed in distilled water in which the additive, 0.25% lithium fluoride (LiF, 99.98%, Alfa Aesar) had been dissolved. The contribution of LiF as sintering additive to spinel sintering and YAG sintering was discussed in our previous papers [6,11]. Excess Li released from the additive is incorporated in the ceramic YAG matrix, substitutes for higher positive valence Y and/or Al cations and as a result of charge equilibrium requirements, generates oxygen vacancies. After water evaporation and drying using a freeze dry apparatus (Freezone1, LABCONCO Inc., Kansas City, MO), the powder was inserted into the 25 mm diameter graphite die of the SPS apparatus (FCT-HP D5/1), which was covered with 20 mm thick graphite wool for thermal insulation.

The temperature was measured by a pyrometer focused on the upper graphite punch, 5 mm above the sintered sample. Several different sintering regimes were examined, in order to determine the effect of SPS processing parameters on the final density and the functional property of the Nd:YAG specimens. The processing parameters included the sintering temperature of the SPS treatment in the 1200–1400 °C range, the holding time at the sintering temperature (1–120 min) and the heating rate to the sintering temperature (2–100 °C/min). A constant axial pressure (64 MPa) was applied at a relatively elevated temperature 1000 °C, at which the vapor pressure of the LiF additive is sufficiently high to allow its easy escape from the bulk sample. The effect of the LiF additive was examined by having each treatment applied both to LiF-free powder and to the LiF doped one. The samples thickness varies from 2 to 3.5 mm after sintering and depends on the amount of powder, which was placed between in the die. The thickness after final polishing is decreased by about 0.5 mm.

Microstructural characterization of the sintered specimens was carried out with a High Resolution Scanning Electron Microscope (SEM) (JEOL®JSM-7400). The grain size distribution was determined from the SEM pictures using the Thixomet™ image analysis software. Approximately 300 grains were used for each data set. Vickers hardness values were determined using a Buehler microhardness tester (MMT-7) under 0.3 kg load. The elastic modulus of the samples was derived from the ultrasonic sound velocity measurements and the measured density. Densities of the sintered specimens were

determined by the Archimedes method. Samples for bending strength measurements by the three point method were prepared by cutting SPS processed specimens into 1.5 mm × 2 mm × 20 mm bars. The tests were conducted in a testing machine (Lloyd Instruments Ltd., UK).

Transmission spectra of the specimens (thickness of 3 mm) were measured in the 400–1000 nm wavelength region, using a spectrophotometer (model: V-1100D). A special home-built set up was used for the IR wavelengths up to 5800 nm. The light source was a tungsten halogen lamp of 250 W power. The light was mechanically chopped at 140 Hz using TTT C995 chopper controller. Horiba FHR640 monochromator with 1.2 nm/mm spectral dispersion (for 1200 grooves/mm grating) provided the spectral separation using 300, 600, 1200 grooves/mm gratings, and a InSb photodiode cooled at 77 K was used as a detector. The signals were amplified using SR 7265 DSP amplifier and the data was recorded using a LabVIEW program.

3. Results and discussion

The large amount of the collected data is presented in the form of graphs, which in some cases, are accompanied by appropriate micrographs. Cross effects between the different processing parameters when observed are pointed out and discussed.

3.1. Density and grain size

Density is usually the first material property, examined at the outcome of powder consolidation. The relative density of both the LiF-free and the LiF-doped samples as a function of the holding time at 1400 °C peak temperature is shown in Fig. 1a for two widely different heating rates, namely 5 °C/min and 100 °C/min. Data illustrate the significant effect of the presence of the LiF additive on the required holding time at the sintering temperature. Similar results were obtained for the previously studied spinel [10,11] and YAG [6] ceramics. The samples with the LiF addition attained quasi full density as soon as the apparatus reached the sintering temperature. In contrast, the LiF-free samples required an additional of 60 min holding time in order to attain full density. The heating rate affects only slightly the relative density, even though a lower heating rate actually implies a more extended integrated sintering time. The treatments shown in Fig. 1b are carried in the 1200–1400 °C temperature range with a heating rate of 5 °C/min and holding time of 20 min. The effect of the LiF presence on the density is further illustrated by the full density reached in the LiF doped sample treated at 1200 °C, whereas the undoped sample reached only 95% relative density at this temperature.

Full density is attained even in the undoped samples at 1400 °C. Transparent YAG processed by conventional sintering in the presence of additives or by the two step sinter-HIP approach requires processing temperature of the order of 1700 °C. The substantially reduced sintering temperature in the course of the SPS treatment constitutes one of the main advantages of the latter.

3.2. Grain size

Grain size, like densification, is a transport dependent property and is significantly affected by the presence of the LiF additive. In the LiF doped sample, raising the sintering temperature from 1200 °C to 1400 °C with a holding time of 20 min at each temperature and for a 2 °C/min heating rate, increases the grain size from 0.8 to 3.1 μm, whereas in the undoped sample the grain size stays below 0.5 μm (Fig. 2a). The dependence of the grain size of the Nd:YAG samples on the holding time at 1400 °C for two heating rate 5 and 100 °C/min is illustrated in Fig. 2b. Holding time of 120 min at 1400 °C temperature causes an additional grain growth in the doped sample to 6.5 μm (heating rate 5 °C/min), while the grain size is unaffected in the undoped sample. The remarkable grain growth in the doped samples treated at low heating rate is attributed to LiF dissolution within the Nd-YAG particles during prolonged heating to the temperature at which LiF starts to evaporate (900–1000 °C) and to its effect on mass transfer at higher temperatures.

The microstructure of fully dense doped and undoped specimens is shown in Fig. 3.

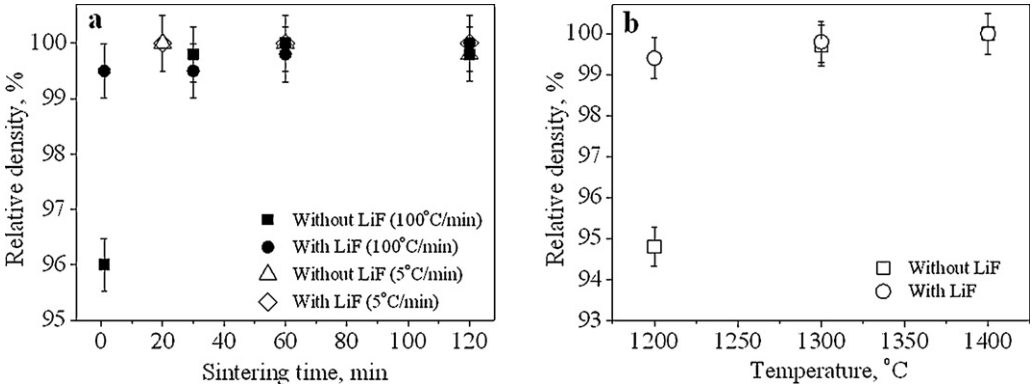

Fig. 1. Relative density of the Nd:YAG: (a) as a function of the holding time at 1400 °C; (b) as a function of the temperature for heating rate 5 °C/min and holding time 20 min.

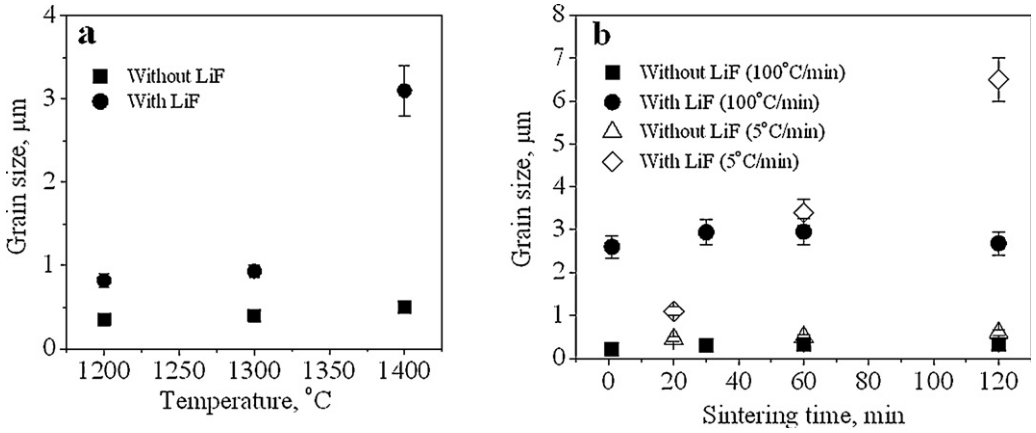

Fig. 2. The effect of temperature (a) and sintering time (b) on the grain size of the LiF-doped and undoped Nd:YAG specimens sintered at various heating rates.

The microstructure of both LiF-free and in LiF-doped YAG, is much finer than of the corresponding spinel samples treated under similar conditions. This difference reflects the different crystal structure of the two ceramics. The spinel structure has a large number of empty interstitial sites (only 1/2 of the octahedral sites and 1/8 of the tetrahedral sites are occupied by Mg and Al cations), while YAG has a more closely packed structure. The accelerated mass transport effects may be accounted for by either the different crystal structure and/or by the different mobility of the rate determining species. Whereas it is well established that oxygen is the rate determining species in spinel [10], the prevalent view leads to a different conclusion with regard to YAG. According to creep rate [21] and diffusion [22] studies, the diffusion of Y^{3+} and a possible Nd^{3+} cations are rate determining, while on the basis of the experimental investigation of grain boundary grooving [23] oxygen anions determine mass transport. Beyond dispute, however, is the observation that in both ceramics, the presence of LiF greatly accelerates mass transport. The presence of LiF has been linked to the generation of excess oxygen vacancies, it thus seems likely that oxygen does play a certain role in Nd:YAG grain growth also.

3.3. Mechanical properties

The collected data on hardness and bending strength values are presented in Fig. 4.

Hardness reaches its final values within 20 min holding time both in the undoped and in the LiF-doped samples. Not unexpectedly, hardness correlates with the grain size. The undoped Nd:YAG samples with submicron grain size display hardness values of about 1570 ± 30 HV. The LiF-doped samples with their larger grain size display lower hardness values around 1460 ± 30 HV. The other processing parameters exert little, if any, effect, on the observed hardness.

The bending strength displays, like the hardness, higher values in the undoped than in the doped samples (420 ± 18 MPa vs. 310 ± 28 MPa). It is noteworthy that in both samples, the final bending strength values are reached progressively only after 2 h holding time at 1400 °C.

The Young modulus both in the doped and the undoped Nd:YAG sample processed at 1400 °C reaches the maximal value of about 286 ± 5 GPa (Fig. 5). The difference between the Young modulus in the doped vs. undoped sample, reflects the difference of their relative density as a function of the processing parameters.

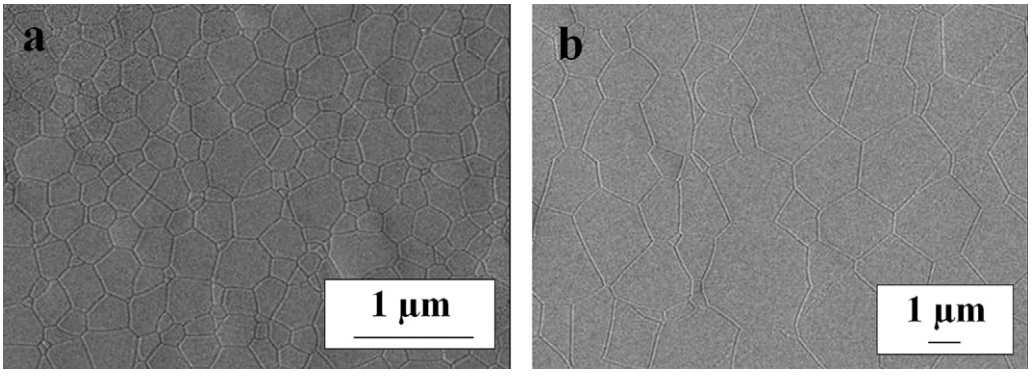

Fig. 3. Optical images of undoped (a) and doped (b) Nd:YAG fully dense specimens.

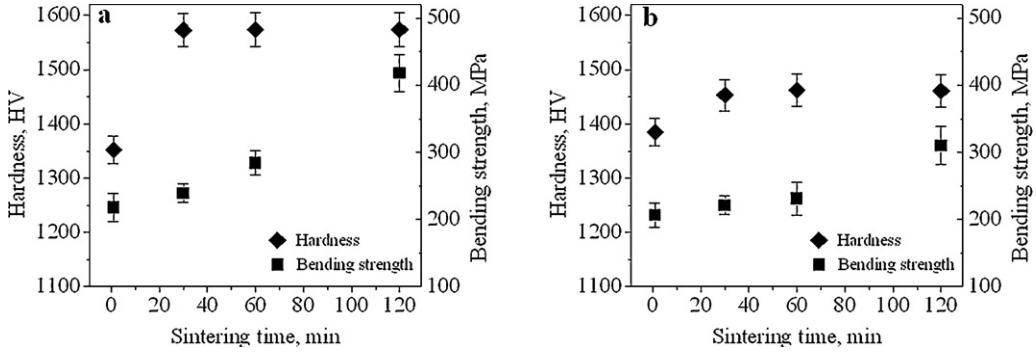

Fig. 4. The mechanical properties of (a) undoped and (b) LiF-doped Nd:YAG specimens as a function of sintering time, sintered at 1400 °C.

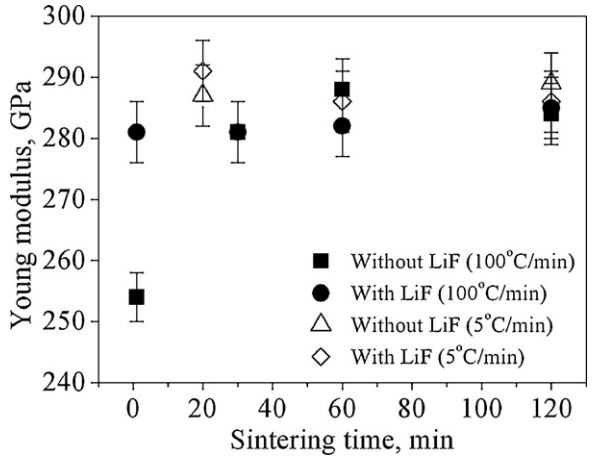

Fig. 5. The Young modulus of LiF doped and undoped Nd:YAG samples, SPS treated at two different heating rates.

3.4. Optical transmittance

As mentioned above, the transmittance over the visible and IR range is among the important functional properties of transparent ceramics including Nd:YAG. The analysis of the dependence of transmittance on the various processing parameters is, however, less straightforward than for the structural and for the mechanical properties. The transmittance is severely affected by the presence of residual pores; the latter also decrease the relative density. Grain size is known to affect optical transmittance in a manner that is wavelength dependent. Finally, and that may be the most critical parameter in an SPS environment, the carbon containing atmosphere that prevails in the chamber impairs severely the optical transmittance.

The transmittance in the optical and IR wavelength range for a LiF-doped sample SPS treated at 1400 °C for 20 min is shown in Fig. 6.

The SPS processing parameters act on the transmittance of the undoped samples in a consistent manner. Higher holding temperature, longer heating time and slower heating rate (i.e. longer integrated sintering time) improved the transmittance, at least within the range of the processing parameters examined in the course of the present study (Fig. 7).

The transmittance spectra of both LiF-doped and undoped samples in the 300–1200 nm wavelength are shown in Fig. 8. The transmittance of a reference sapphire sample and the difference transmittance between the doped and undoped Nd-YAG specimens are also shown. The spectra illustrate the significantly enhanced transmittance values in up to 500 nm wavelength in samples that had been consolidated in the presence of the LiF additive. Transmittance values close to 80% are found in the LiF doped samples, with thickness of 3 mm, after a 20 min treatment at 1400 °C, whereas even after a

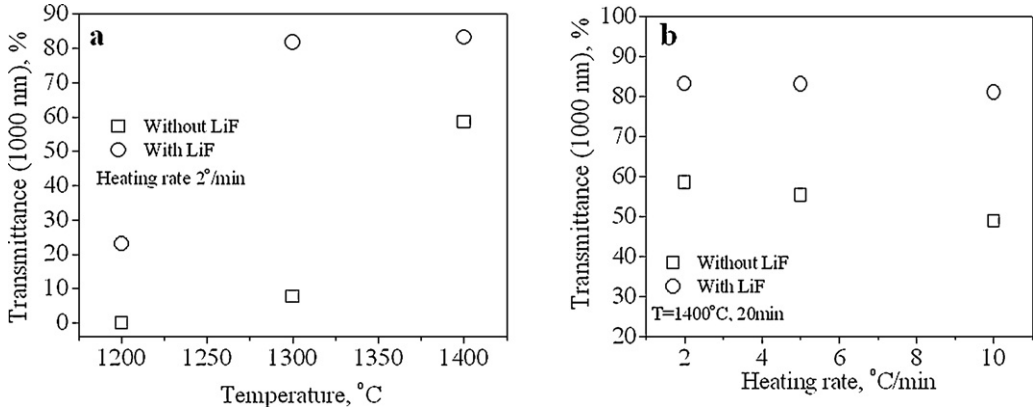

Fig. 6. Transmittance at 1000 nm wavelength of LiF-doped and undoped Nd:YAG specimens (thickness of 3 mm), sintered at (a) various temperatures and (b) different heating rates.

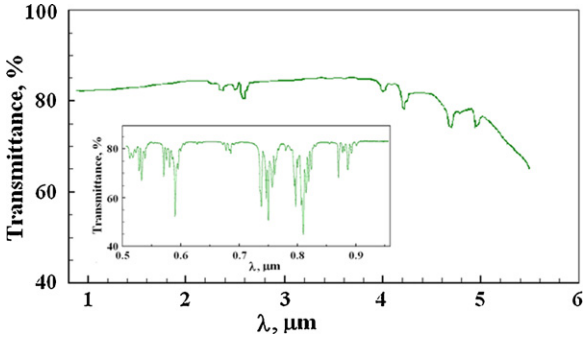

Fig. 7. Optical transmittance of the LiF-doped specimen sintered at 1400 °C for 20 min at a heating rate 2 °C/min, the insert shows the details of the optical transmittance in the low wavelength range (<1 μm) of the spectrum.

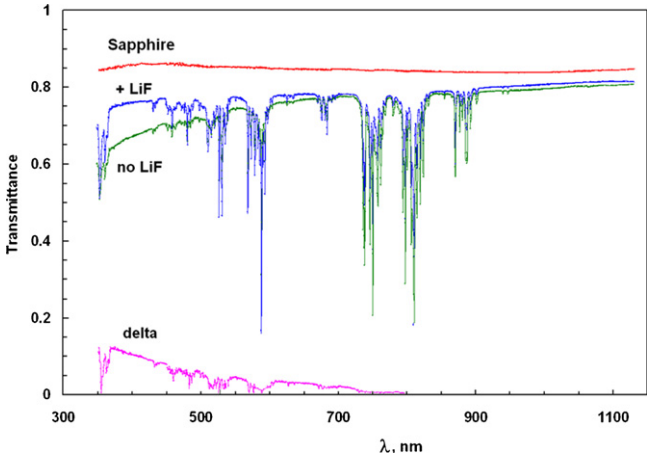

Fig. 8. Transmittance of the SPS-treated Nd:YAG samples, LiF-doped and undoped. The transmittance of a sapphire sample and the transmittance difference (delta) between the doped and undoped Nd-YAG specimens are also shown.

1400 °C treatment, namely at full density, the LiF-free specimen exhibits only a much lower, 65%, transmittance value. It is also significant that the presence of the additive does not seem to affect the absorption peaks of the Nd dopant.

The increased absorption in the undoped samples may be attributed either to a large concentration of residual submicron pores and/or to carbon contamination. The presence of residual occluded pores and of residual voids at triple points in the undoped sample is shown in Fig. 9a and b. In contrast, the LiF-doped sample displays very clean grain boundaries as shown in Fig. 10. It is noteworthy that the pores are substantially smaller than the parent grains, the serrated aspect of the grain boundary in the lower part of Fig. 9b may be due to its being a low angle boundary generated by a network of dislocations.

The effect of the LiF additive is two-fold; it acts as a cleansing agent and assists in eliminating the carbon contamination. It is also a grain boundary movement accelerator as attested by the six-fold increase of the average grain size in the LiF doped samples, as compared to the undoped ones. In the course of the grain-growth, the moving grain boundaries drag along and eliminate the pores.

We attribute the enhanced transmittance of the LiF-doped samples in the low wavelength region of the spectrum to the combined effect of pore elimination and carbon cleansing. It is also gratifying that the presence of the additive does not affect to any perceivable manner the absorption in the low wavelength range of the spectrum.

Thus, the results confirm that the presence of a small concentration of LiF additive has a significant effect on the transparency of the Nd:YAG samples at the outcome of the SPS treatment. Similar results were observed in SPS consolidated spinel [11] and YAG [6] samples and were attributed to the reaction of the carbon with the fluorine atoms, that leads to the formation of volatile (CF)n species. The latter are expulsed from the bulk as long as open channels are still available prior the last consolidation stages.

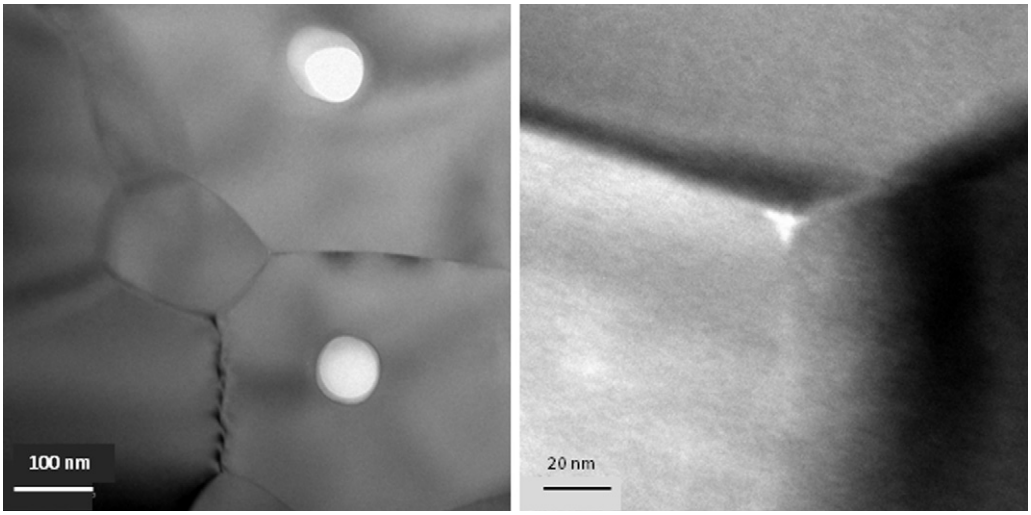

Fig. 9. (a) TEM micrograph of an undoped Nd:YAG sample showing the presence of occluded nano-pores and non-straight grain boundary along which impurities may have segregated. (b) nano-void at a triple junction.

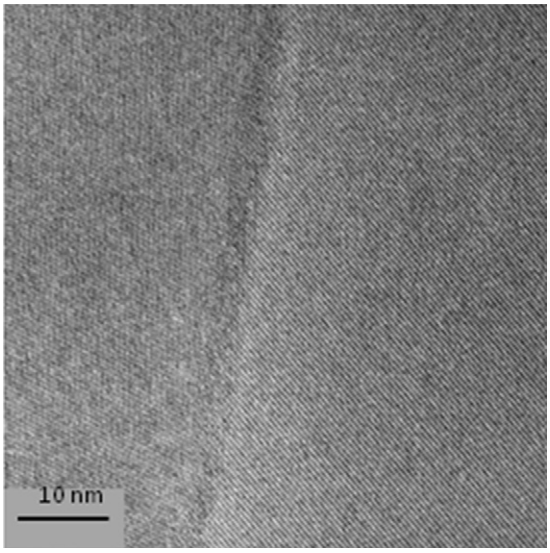

Fig. 10. High resolution TEM micrograph of the clean grain boundary in the LiF-doped Nd-YAG sample.

4. Conclusions

Transparent 1 at.% Nd:YAG ceramics were fabricated by SPS processing from nanometric Nd:YAG powders, both undoped and in the presence of an 0.25% LiF additive. The mechanical and optical properties of the consolidated samples were determined as a function of the processing parameters, namely holding time, sintering temperature and heating rate.

The presence of the LiF additive affects mass transport, accelerates the densification and the grain growth in the course of the SPS process. The grain size in the LiF doped Nd:YAG is increased by an order of magnitude with respect to that in the undoped samples.

Hardness and bending strength are lowered in the presence of the LiF additive, in consistence with the increased grain size. The Young modulus is relatively unaffected by variation of the processing parameters.

The optical transmittance in the LiF doped samples is significantly higher as compared to the undoped ones. An optical transmittance of close to 80% at the wavelength 1000 nm (97% of the theoretical transmission) was obtained for a specimen containing 0.25 wt.% LiF, sintered at 1400 °C at a 2 °C/min heating rate and a holding time 20 min. Under similar conditions the transmittance of the undoped samples was of the order of 60%. The increased optical transmittance of the doped samples, processed in the carbon rich SPS environment, is attributed to a possible cleansing effect of the fluorine component of the additive, which by combining with carbon forms volatile species that are expelled as long as the open channels subsist in the samples undergoing consolidation.

References

[1] R. Orrù, R. Licheri, A.M. Locci, A. Cincotti, G. Cao, Consolidation/synthesis of materials by electric current activated/assisted sintering, Materials Science and Engineering Reports 63 (2009) 127–287.

[2] A. Ikesue, K. Yoshida, Influence of pore volume on laser performance of Nd:YAG ceramics, Journal of Materials Science 34 (1999) 1189–1195.

[3] R. Fedyk, D. Hreniak, W. Łojkowski, W. Stręk, H. Matysiak, E. Grzanka, S. Gierlotka, P. Mazur, Method of preparation and structural properties of transparent YAG nanoceramics, Optical Materials 29 (2007) 1252–1257.

[4] S. Nakamura, H. Yoshioka, Y. Matsubara, T. Ogawa, S. Wada, Efficient tunable Yb:YAG ceramic laser, Optics Communication 281 (2008) 4411–4414.

[5] S. Lee, E.R. Kupp, A.J. Stevenson, J.M. Anderson, G.L. Messing, X. Li, E.C. Dickey, J.Q. Dumm, V.K. Simonaitis-Castillo, G.J. Quarles, Hot isostatic pressing of transparent Nd:YAG ceramics, Journal of the American Ceramic Society 92 (2009) 1456–1463.

[6] N. Frage, S. Kalabukhov, N. Sverdlov, V. Ezersky, M.P. Dariel, Densification of transparent yttrium aluminum garnet (YAG) by SPS processing, Journal of the European Ceramic Society 30 (2010) 3331–3337.

[7] R. Chaim, M. Kalina, J.Z. Shen, Transparent yttrium aluminum garnet (YAG) ceramics by spark plasma sintering, Journal of the European Ceramic Society 27 (2007) 3331–3337.

[8] C. Rachman, Densification mechanisms in spark plasma sintering of nanocrystalline ceramics, Materials Science and Engineering: A 443 (2007) 25–32.

[9] R. Chaim, R. Marder, C. Estournès, Optically transparent ceramics by spark plasma sintering of oxide nanoparticles, Scripta Materialia 63 (2010) 211–214.

[10] N. Frage, S. Cohen, S. Meir, S. Kalabukhov, M. Dariel, Spark plasma sintering (SPS) of transparent magnesium–aluminate spinel, Journal of Materials Science 42 (2007) 3273–3275.

[11] S. Meir, S. Kalabukhov, N. Froumin, M.P. Dariel, N. Frage, Synthesis, Densification of transparent magnesium aluminate spinel by SPS processing, Journal of the American Ceramic Society 92 (2009) 358–364.

[12] R. Marder, R. Chaim, G. Chevallier, C. Estournès, Effect of 1 wt.% LiF additive on the densification of nanocrystalline Y_2O_3 ceramics by spark plasma sintering, Journal of the European Ceramic Society 31 (2011) 1057–1066.

[13] A. Ikesue, Y.L. Aung, Ceramic laser materials, Nature Photonics 2 (2008) 721–727.

[14] W. Liu, B. Jiang, W. Zhang, J. Li, J. Zhou, D. Zhang, Y. Pan, J. Guo, Influence of heating rate on optical properties of Nd:YAG laser ceramic, Ceramics International 36 (2010) 2197–2201.

[15] S. Kochawattana, A. Stevenson, S. Lee, M. Ramirez, V. Gopalan, J. Dumm, V.K. Castillo, G.J. Quarles, G.L. Messing, Sintering and grain growth in SiO_2 doped Nd:YAG, Journal of the European Ceramic Society 28 (2008) 1527–1534.

[16] X. Li, Fabrication of transparent yttrium aluminum garnet ceramic, Journal of Physics: Conference Series 152 (2009) 012079.

[17] R. Chaim, Z. Shen, Grain size control by pressure application regime during spark plasma sintering of Nd-YAG nanopowders, Journal of Materials Science 43 (2008) 5023–5027.

[18] U. Aschauer, P. Bowen, Theoretical assessment of Nd:YAG ceramic laser performance by microstructural and optical modeling, Journal of the American Ceramic Society 93 (2010) 814–820.

[19] K. Morita, B. Kim, H. Yoshida, K. Hiraga, Spark-plasma-sintering condition optimization for producing transparent $MgAl_2O_4$ spinel polycrystal, Journal of the American Ceramic Society 92 (2009) 1208–1216.

[20] K. Morita, B. Kim, H. Yoshida, K. Hiraga, Densification behavior of a fine-grained $MgAl_2O_4$ spinel during spark plasma sintering (SPS), Scripta Materialia 63 (2010) 565–568.

[21] M. Jiménez-Melendo, H. Haneda, H. Nozawa, Ytterbium cation diffusion in yttrium aluminum garnet (YAG) implications for creep mechanisms, Journal of the American Ceramic Society 84 (2001) 2356–2360.

[22] R. Boulesteix, A. Maître, J.-. Baumard, Y. Rabinovitch, C. Sallé, S. Weber, M. Kilo, The effect of silica doping on neodymium diffusion in yttrium aluminum garnet ceramics: implications for sintering mechanisms, Journal of the European Ceramic Society 29 (2009) 2517–2526.

[23] M.I. Peters, I.E. Reimanis, Grain boundary grooving studies of yttrium aluminum garnet (YAG) bicrystals, Journal of the American Ceramic Society 86 (2003) 870–872.